Preprints.org

Article

MSC Sheet Assembly Duration Correlates with Extracellular Matrix Deposition, but Not Proliferative Activity or Donor Features

Valentina Sergeevna Glazyeva , Natalya Andreevna Alexandrushkina , Peter Petrovich Nimiritsky ,
Maria Aleksandrovna Kulebyakina , Roman Yurievich Eremichev , Pavel Igorevich Makarevich [*]

Article

MSC Sheet Assembly Duration Correlates with Extracellular Matrix Deposition, but Not Proliferative Activity or Donor Features

Valentina S. Glazyeva [2,†], **Natalya A. Alexandrushkina** [1,2,†], **Peter P. Nimiritsky** [1,2], **Maria A. Kulebyakina** [2], **Roman Yu. Eremichev** [1,2] **and Pavel I. Makarevich** [1,2,*]

1. Institute for Regenerative Medicine, Medical Research and Education Center, Lomonosov Moscow State University, 27-10, Lomonosovskiy av., Moscow 119192, Russia;
2. Faculty of Medicine, Lomonosov Moscow State University, 27-1, Lomonosovskiy av., Moscow 119192, Russia;
* Correspondence: pmakarevich@mc.msu.ru
† these authors contributed equally.

Abstract: Cell sheet (CS) engineering using human MSC is of significant interest for regenerative medicine and this rapidly growing field translates to clinical use in a number of indications. Nevertheless, little is known of factors that define the timing of CS assembly from primary cultures which is important for planning treatments in both – autologous and allogeneic modes of use. We used a comparative *in vitro* approach with primary donors' (n=14) adipose-derived MSC and evaluated the impact of healthy subject's characteristics (age and sex), MSC culture features (population doubling time and lag-phase) and extracellular matrix (ECM) composition along with factors related to connective tissue formations (α-SMA and FAP-α) on CS assembly duration. Using qualitative and quantitative analysis methods we found that in seeded MSC high contents of collagen I and collagen IV had a direct correlation with longer CS assembly duration. In contrary, shorter lag-phase cultures yielded ready-to-use CS faster while age, sex, fibronectin, laminin, α-SMA and FAP-α failed to provide significant correlations with timing of assembly. We also found that in detachable CS FAP-α was negatively correlated with duration of assembly suggesting that its concentration might be rising over time and contribute to MSC activation, transition to α-SMA-positive myofibroblasts and ECM deposition/turnover.

Keywords: cell sheet; tissue engineering; mesenchymal stromal cells; extracellular matrix; fibroblast activating protein; myofibroblast

1. Introduction

Cells used for cell therapy readily undergo cell death due to anoikis during injection [1] and immediately after transplantation into damaged tissue [2]. To overcome this challenge hindering efficacy of therapy cell sheet (CS) technology was developed by T. Okano as a delivery method using tissue engineering devoid of synthetic scaffolds or animal-based carrier materials [3]. CS are minimal tissue constructs comprising of viable adherent cells bound by extracellular matrix (ECM) produced by these cells over time *in vitro.* Besides ECM MSC sheets can also bear soluble growth factors, cytokines and extracellular vesicles trapped within matrix meshes [4].

After transplantation within CS cells preserve their activity and retain at the site of application for a significant period of time ranging from days to weeks. Contrasting to widely used spheroids cells in CS have access to relatively evenly distributed nutrients and oxygen providing homogeneous conditions for all cellular elements [5,6].

CS from mesenchymal stem/stromal cells (MSC) of different tissue origin gained significant attention as a method for tissue engineering in regenerative medicine. Multipotency of MSC and rich ECM composition are properties that made MSC sheets a valuable utility to treat connective tissue

defects (e.g., bone fractures, cartilage degeneration), mucosal ulcers, skin lesions and cardiac disease [7]. Prospects of CS from MSC are beyond doubt yet certain practical challenges may limit widespread use of this technology.

One critical point is related to standardization of CS assembly that may take from 3 to 15 days to be obtained from harvested primary MSC. Heterogeneity of MSC features as well as donors' features (age, sex, comorbidity) may affect the MSC properties and determine efficacy of CS assembly. Furthermore, human tissue material (bone marrow, subcutaneous or visceral fat) yields a heterogeneous pool of primary cells even when commercial reagents or GMP protocols of isolation and culture are used [8]. Eventually, one may fail to obtain a ready-to-use CS within a specific time frame – e.g. by the day of planned surgery or as soon as possible in burn or emergency trauma patients. We failed to find published studies providing insights into feasibly evaluated determinants that impact CS assembly duration indicating a gap of knowledge that may be of importance for practical application of this approach.

2. Materials and Methods

2.1. Human adipose tissue MSC source and culture

Previously characterized human adipose-derived MSC isolated from voluntary donors (n=14) were obtained from the National depositary bank of living systems (Lomonosov Moscow State University, Russia). All procedures with tissue samples from patients were performed in accordance with the Declaration of Helsinki and approved by the Local Ethical Committee, Medical Research, and Education Center, Lomonosov Moscow State University (IRB00010587), protocol #4 (2018). Samples of human adipose-derived MSCs were collected from the Cryobank of the Institute for Regenerative Medicine of Lomonosov Moscow State University (collection ID MSC_AD_MSU, www.human.depo.msu.ru). Vials were thawed and cells were transferred to a tube with DMEM/F12 medium (Gibco, USA) supplemented with 10% fetal bovine serum (FBS; HyClone, USA), 100 U/ml of penicillin and 100 µ/ml streptomycin (Gibco, USA). Cells were centrifuged (5 minutes, 200 g) to remove dimethyl sulfoxide (DMSO); supernatant was aspirated, cell pellet was resuspended in complete DMEM/F12 (10% FBS) and seeded at 5×10^3 cells/cm² to culture dishes (Corning, USA). Cells were cultured under standard conditions (37° C and 5% CO_2) with a change of medium every 2-3 days and passaged at 80–90% of density cells using 0.05% Trypsin/EDTA solution (Gibco, USA) at 1:3 ratio.

2.2. Timelapse monitoring of MSC cultures

Proliferation analysis was performed using IncuCyte® Live Cell Analysis System (Essen Bioscience, USA). Cells were seeded to 12-well plates (Corning, USA) at 5×10^3 cells/cm² for 96 hours. Timelapse images were captured every 4 hours to plot growth curves reflecting confluency (percentage of area occupied by cells) in each well of a 12-well plate. Using obtained micrographs of each MSC culture we analyzed cell morphology over time and determined the duration of lag-phase. More than two mitotic divisions in the field of view (10x objective) indicated the end of the lag-phase and onset of subsequent exponential growth phase. Population doubling time (PDT) of MSC was calculated for each cell culture at the stage of exponential growth by dividing the natural logarithm of 2 by the exponent of growth.

2.3. Assembly of cell sheets from MSC

For Reader's convenience schematic of described experiments is provided in Supplementary Figure 1. Assembly protocol for tissue-engineered constructs from MSC involves a long-term culture in complete growth medium until constructs that can be freely detached from the culture plastic. MSC were seeded to uncoated culture plastic at 50×10^3 cells/cm² in complete growth medium (DMEM/F12, 10% FBS) supplemented with ascorbic acid (50 µg/mL) and cultured with medium replacement every 2 days for up to 11 days [9]. We suggested spontaneous detachment of CS as an objective endpoint of assembly completion. Briefly, using daily observations we evaluated CS

assembly duration as number of days after seeding until spontaneous detachment of CS. We used parallel monolayer cultures and undetached CS specimen for histology and protein assays. Majority of monolayer cultures were analyzed at Days 2-4 upon reaching confluency. CS assembly duration varied between donors showing median duration of 8 days with a minimum of 5 and maximum of 11 days.
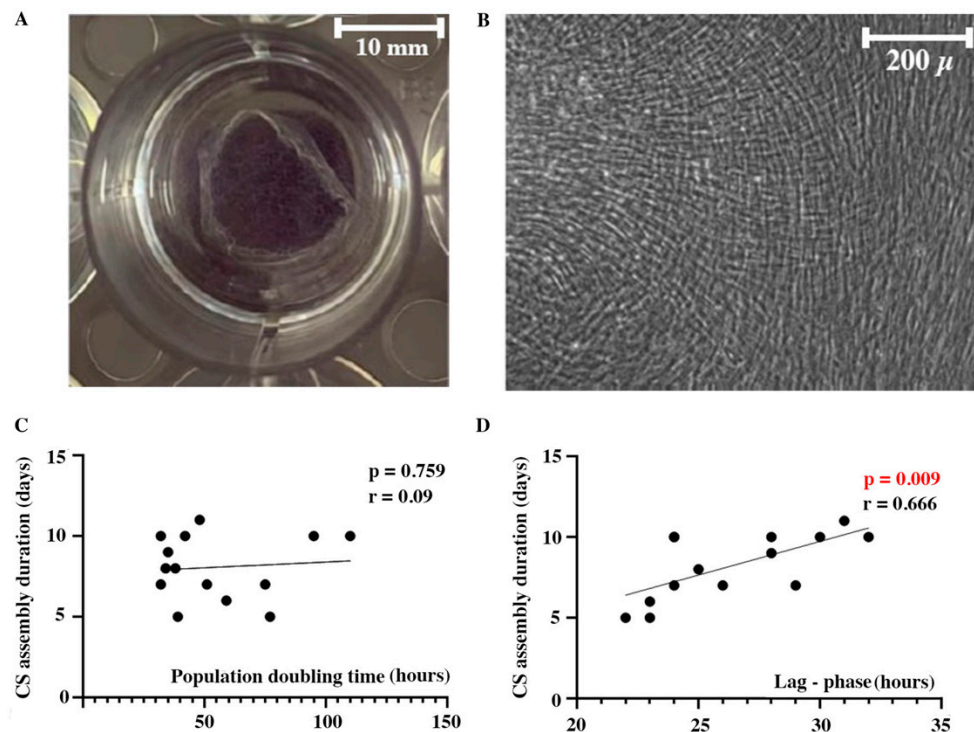

Figure 1. Cell sheets morphology and correlation of cultural characteristics with assembly duration. Macro photo of CS after partial detachment from a 12-well plate well (A) and representative micrograph of CS from human adipose tissue MSC (B) demonstrating cell morphology (phase contrast microscopy). Dotted plots represent Pearson correlations of CS assembly duration with population doubling time (C) and lag-phase (D) after seeding.

2.4. Immunolabeling procedures

For immunofluorescent labeling the MSC sheets or monolayers were washed three times by warm PBS and fixed with 4% formaldehyde in PBS for 10 minutes. For labeling of intracellular proteins cultures were permeabilized with 0.2% Triton X-100 for 10 minutes and washed three times with PBS for 5 minutes. Blocking was done by 1% bovine serum albumin (BSA) with addition of 10% non-immune serum of secondary antibodies donor. After blocking the samples were incubated overnight at 4°C with primary rabbit polyclonal antibodies vs. human collagen I, collagen IV, fibronectin, α-SMA or laminin (all from Abcam, UK) at 1:300 dilution in blocking buffer. Afterwards the samples were washed three times with PBS for 5 minutes and secondary antibodies conjugated with Alexa Fluor 488 or Alexa Fluor 594 (Invitrogen, USA) at 1:1000 dilution were added for 1 hour at room temperature. Nuclei were labeled by 4′,6-diamidino-2-phenylindole (DAPI, Sigma-Aldrich, USA) for 30 minutes in the dark and then washed 3 times with PBS for 5 minutes. Image acquisition was performed on DMi8 inverted microscope (Leica Microsystems, Germany).

2.5. Estimation of α-SMA-positive MSC prevalence

Analysis of α-SMA-positive MSC was carried out using the ImageJ program (NIH, USA) in corresponding immunolabeled cultures. Total number of nuclei and the number of α-SMA-positive MSC were counted in micrographs to obtain percentage of α-SMA-positive MSC.

2.6. Protein extraction, dot-ELISA and densitometry

Total protein was extracted from MSC cultures by Laemmli buffer (BioRad, USA). Protein contents within lysates was assayed by Pierce™ BCA Protein Assay Kit (Invitrogen, USA) by manufacturer instructions. Normalization by DNA contents in lysed samples was performed using PicoGreen DNA dye (Thermo Fisher Scientific, USA) as previously described by our group for a similar application to compare MSC sheets and monolayer cultures and account for difference in cell numbers [10]. Due to high molecular weight proteins within ECM of CS we decided to avoid Western blotting and used semi-quantitative analysis of lysates using dot-ELISA. Briefly, lysed samples (1 µl per dot) were pipetted in duplicates to a nitrocellulose membrane and dried at room temperature. Dotted membrane was sliced and corresponding parts were sequentially incubated in 5% non-fat milk solution in PBS containing primary antibodies vs. human collagen I, collagen IV, laminin, fibronectin, α-SMA or FAPα (all from Abcam, UK) at 1:1000 dilution followed by corresponding secondary HRP-conjugated antibody. For normalization we used serially diluted lysates of a known number of cells from a reference MSC culture (ASC52telo, ATCC, USA) which has a stable and detectable production of ECM components [10] and a parallel duplicate membrane was stained by Amido Black dye (Sigma Aldrich, USA).

2.7. Statistical analysis

Data was processed using GraphPad Prizm 8.0.1. and Microsoft Excel software. Descriptive statistics included normality assessment (Shapiro— Wilk test) and calculation of mean and standard error of mean (all data is presented as M±SEM). The differences between the groups were evaluated using Student's t test or Mann—Whitney test. For correlation analysis the Pearson and Spearman linear correlation coefficients were used; all differences and correlations were deemed significant at $p < 0.05$.

3. Results

3.1. Lag-phase duration in seeded MSC culture directly correlates with CS assembly duration

During CS assembly from dense MSC monolayer cells proliferate and accumulate ECM which eventually results in spontaneous detachment once contractile forces within CS overcome adhesion. Ready-to-use CS was a visible construct available for detachment from cultural dish surface without loss of integrity (Figure 1A). All evaluated MSC cultures and resulting CS were morphologically comparable (Figure 1B). Analysis of cultural characteristics demonstrated that CS assembly duration surprisingly did not correlate with proliferation rate of seeded MSC assessed as population doubling time (PDT) (Figure 1C). However, we found a direct correlation of CS assembly duration and seeded MSC lag-phase assessed at early terms of assembly. Lag-phase is a period required for MSC to adhere, flatten and produce ECM to create an environment for proliferation and growth (Figure 1D). Basically, MSC cultures with shortened lag-phase showed faster assembly of CS ready for detachment.

3.2. MSC donor sex or age fail to demonstrate impact on CS assembly duration

We also suggested that donor age and sex might influence MSC proliferative rate and secretory function *in vitro* even in healthy subjects and, thus, define duration of CS assembly. In donor population (n=14) male-to-female distribution was equal with 54:46% respectively with age ranging from 18 to 66 years with a mean of 36±11 years. We found no evidence for sex are age impact on CS assembly duration (Figure 2) - indeed, the youngest (18 years) and the oldest donor (66 years) demonstrated similar time required for CS assembly to be completed (9 days and 7 days respectively) and no statistical significance (r=-0.218; p=0,495) was observed in correlation analysis (Figure 2).
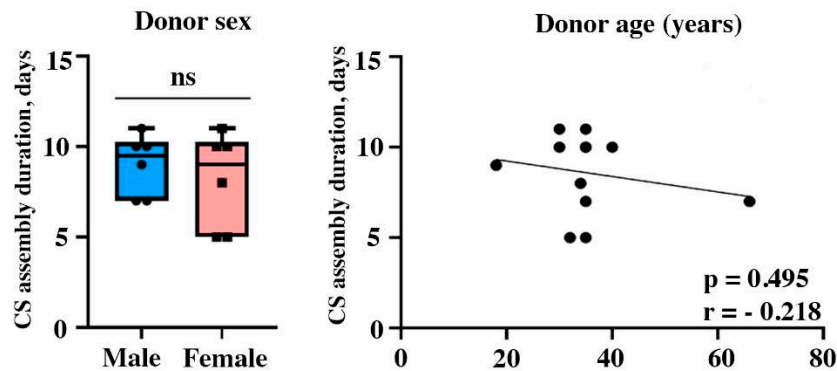
Figure 2. Impact of individual's sex and age on CS assembly duration from primary MSC (dotted plot represents Pearson correlation).

3.3. Collagen I, but not fibronectin contents in seeded MSC directly correlates with increased duration of CS assembly

Matrix deposition rate is considered a significant factor contributing to CS assembly and we performed immunofluorescent visualization of collagen I and fibronectin as major components of ECM. We used dense monolayer formed by Day 2-4 after seeding and attached CS for two histological procedures – with or without permeabilization by Triton X-100. Under non-permeabilized conditions proteins deposited in extracellular compartment are visualized while permeabilization of membranes allows antibody binding with both intra- and extracellular ECM components – thus, permeabilized cultures were termed "total ECM" suggesting that accumulated yet not secreted proteins are visualized as well.

Monolayer MSC demonstrated minimal deposition of collagen I in extracellular space while in assembled CS collagen I was vividly detected in the extracellular part of a non-permeabilized construct demonstrating dramatic accumulation of ECM over time (Figure 3A, "Extracellular ECM"). Using permeabilization we have shown high intracellular content of collagen I in both monolayer MSC and CS indicating ongoing production of ECM even after completion of assembly (Figure 3A, "Total ECM").
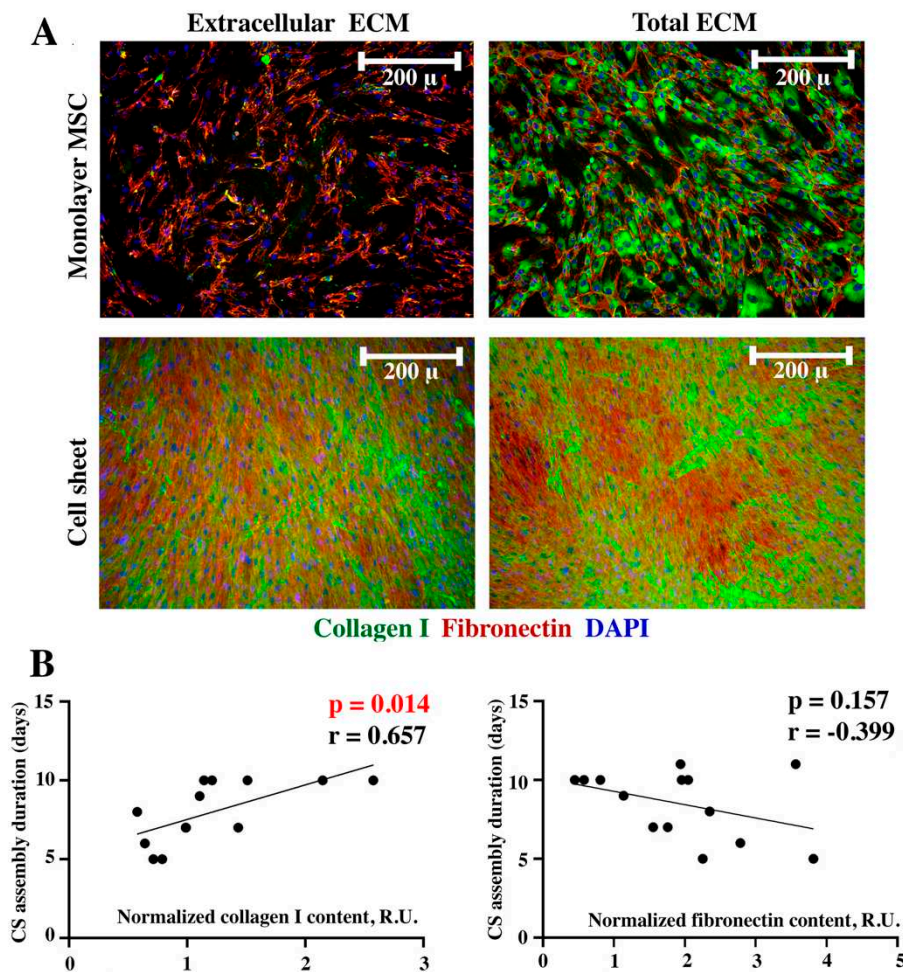
Figure 3. Immunofluorescent labeling of collagen I and fibronectin in monolayer MSC and CS (A) and corresponding Pearson correlation analysis (B) of collagen I or fibronectin content in MSC monolayer and duration of CS assembly.

Fibronectin had bright strand-shaped extracellular deposits in both MSC monolayer and assembled CS (Figure 3A, "Extracellular ECM"). In non-permeabilized monolayer MSC fibronectin deposits were visualized predominantly as a network of thin extracellular filaments (Figure 3A, "Extracellular ECM") while in CS strength of signal was vividly higher covering the field of view. This might also result from CS multilayered structure we have previously shown using confocal microscopy [10–12]. Switching to permeabilization immunolabeling had minimal impact on visualized patterns of fibronectin in both monolayer and CS (Figure 3A, "Total ECM") suggesting its even distribution between intra- and extracellular compartments.

Semi-quantitative analysis we a used dot-ELISA assay for collagen I and fibronectin in lysates obtained from MSC monolayer and ready CS. We found a significant direct correlation (r=0,657; p=0.014) of collagen I relative contents in MSC monolayer and eventual duration of CS assembly from MSC culture of a specific donor (Figure 3B, left plot). Thus, MSC with higher contents of collagen I in monolayer showed a longer CS assembly period. Analysis of fibronectin in MSC showed a non-significant trend (r=-0.399; p=0.157) for an inverse correlation between fibronectin contents and CS assembly duration suggesting that MSC cultures with initial high fibronectin production tend to form a CS faster (Figure 3B, right plot).

3.4. Contents of basement membrane component collagen IV, but not laminin in seeded MSC directly correlates with CS assembly duration

Laminin and collagen IV are typically attributed to basement membrane underlying epithelial cells yet their deposition has a pivotal role in mechanical properties including ECM viscosity and formation of innate tensile forces in tissues [13,14]. Immunofluorescent labeling of laminin using the same approach as described above demonstrated that its extracellular deposition in both MSC monolayer and CS was barely detectable (Figure 4A, "Extracellular ECM"). Sporadic laminin-positive cells with cytoplasmatic signal were attributed to weak permeabilizing impact of 4% paraformaldehyde used for culture fixation. In contrast after permeabilization we found high intracellular accumulation of laminin in both cultures (Figure 4A, "Total ECM"). Thus, laminin was predominantly accumulated inside MSC which was concordant with lack of correlation of its relative amount and CS assembly duration (r=0.414; p=0.159) we found by dot-ELISA (Figure 4B).
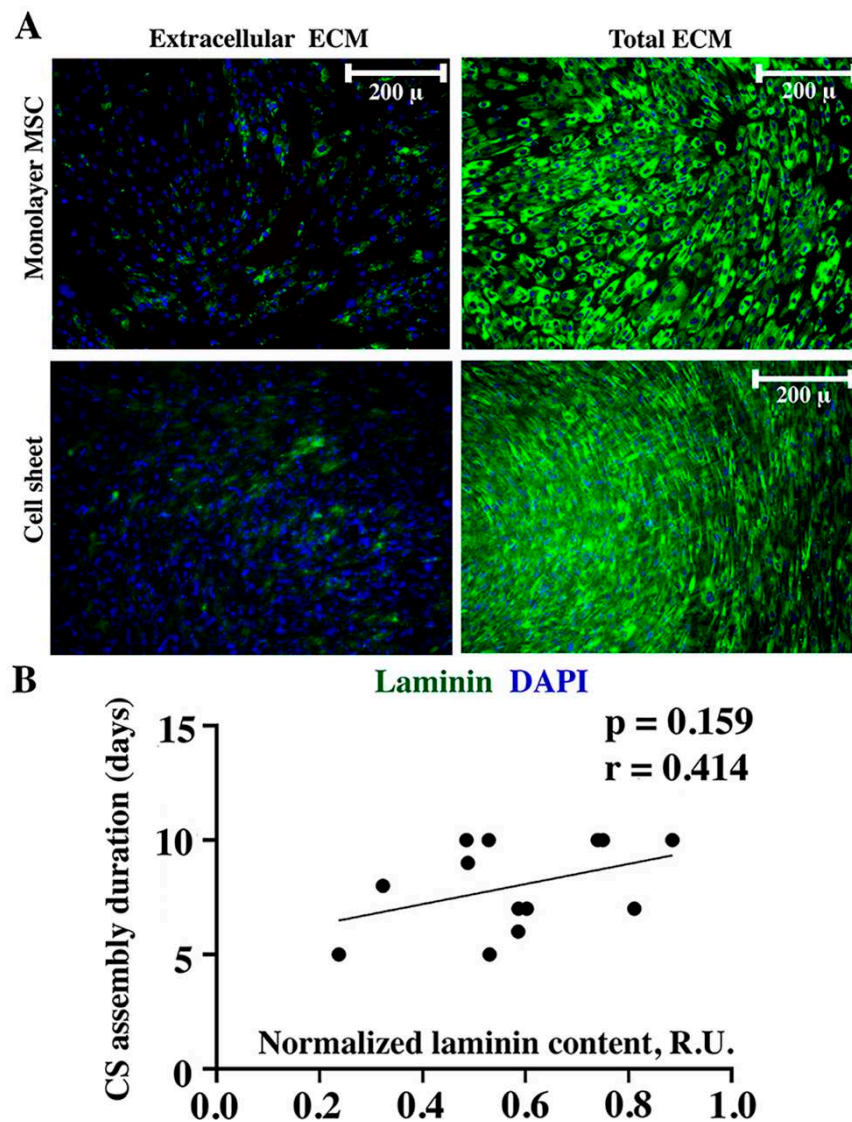

Figure 4. Immunofluorescent labeling of laminin in monolayer MSC or CS (A) and corresponding Pearson correlation analysis (B) of laminin contents in MSC monolayer and duration of CS assembly.

Collagen IV signal in extracellular compartment of monolayer MSC showed low intensity with an increase in a detachable CS (Figure 5A, "Extracellular ECM"). After permeabilization we observed visible accumulation of collagen IV inside the cells in both monolayer and CS which suggested a peculiarly common profile of deposition for two collagens – type IV and type I in monolayer culture characterized by intracellular accumulation and drastic increase of its amount once CS is formed ("Total ECM" in Figure 5A and Figure 3A respectively). Dot-ELISA results demonstrated a direct correlation (r=0.72; p=0.007) of collagen IV relative contents with CS assembly duration indicating that MSC with high production of this ECM component took longer to form a CS (Figure 5B).
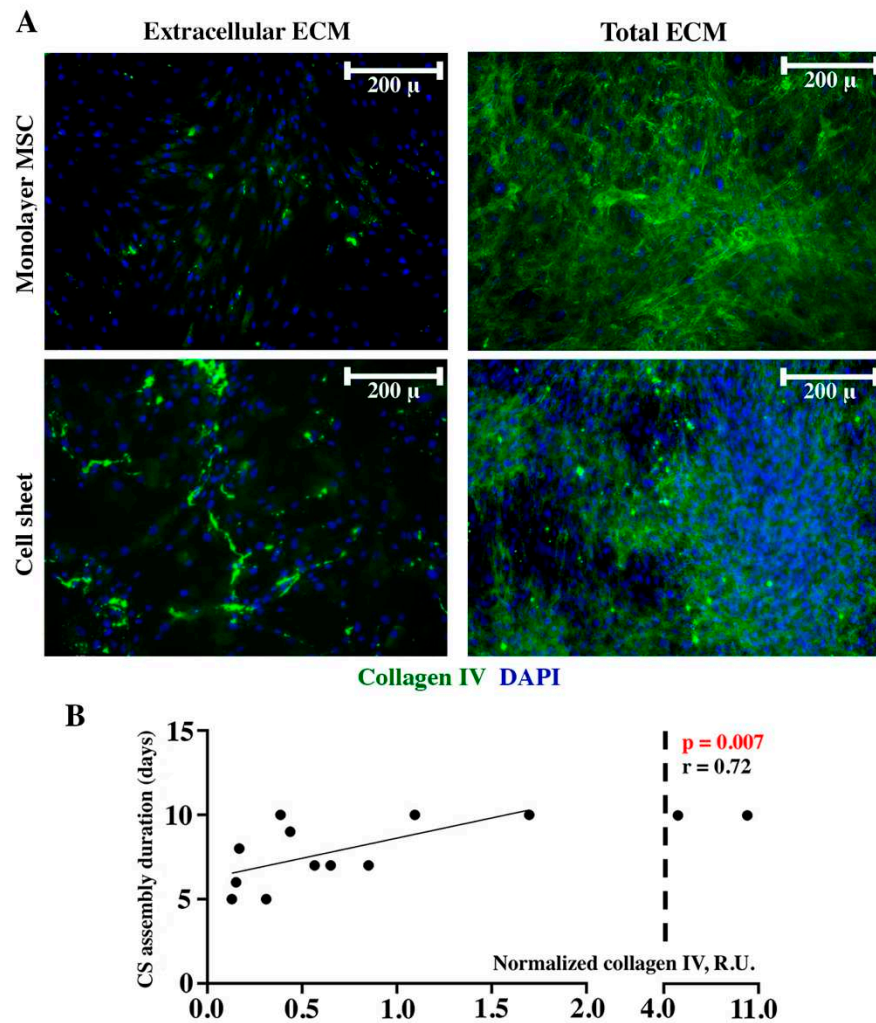
Figure 5. Immunofluorescent labeling of collagen IV in monolayer MSC or CS (A) and corresponding Pearson correlation analysis of collagen IV contents in MSC monolayer lysate and CS assembly duration.

3.5. Factors related to connective tissue do not correlate with assembly duration yet may play a role in assembled CS structure support

3.5.1. Prevalence of α-SMA-positive cells and α-SMA contents fail to correlate with CS duration assembly

Among cells that actively produce ECM and may induce connective tissue formation myofibroblasts are of pivotal importance. Furthermore, MSC may undergo differentiation to myofibroblasts under certain conditions including spontaneous conversion *in vitro* [12]. We evaluated α-smooth muscle actin (α-SMA) as an intracellular marker of myofibroblast phenotype in monolayer MSC and assembled CS. We found a drastic increase of α-SMA-positive MSC in CS which may contribute to contraction and detachment used as study's visual endpoint. This was supported by manual counts of α-SMA-positive cells using DAPI-stained nuclei as an additional cue (Figure 6A). However, correlation analysis of CS assembly duration and α-SMA contents measured by dot-ELISA (Figure 6B) or α-SMA-positive cells counts (Figure 6C) have failed to detect significant relationships between assessed parameters. Thus, despite obvious increase of α-SMA-positive cells over time we found no evidence for its potential role in defining time required for CS maturation.
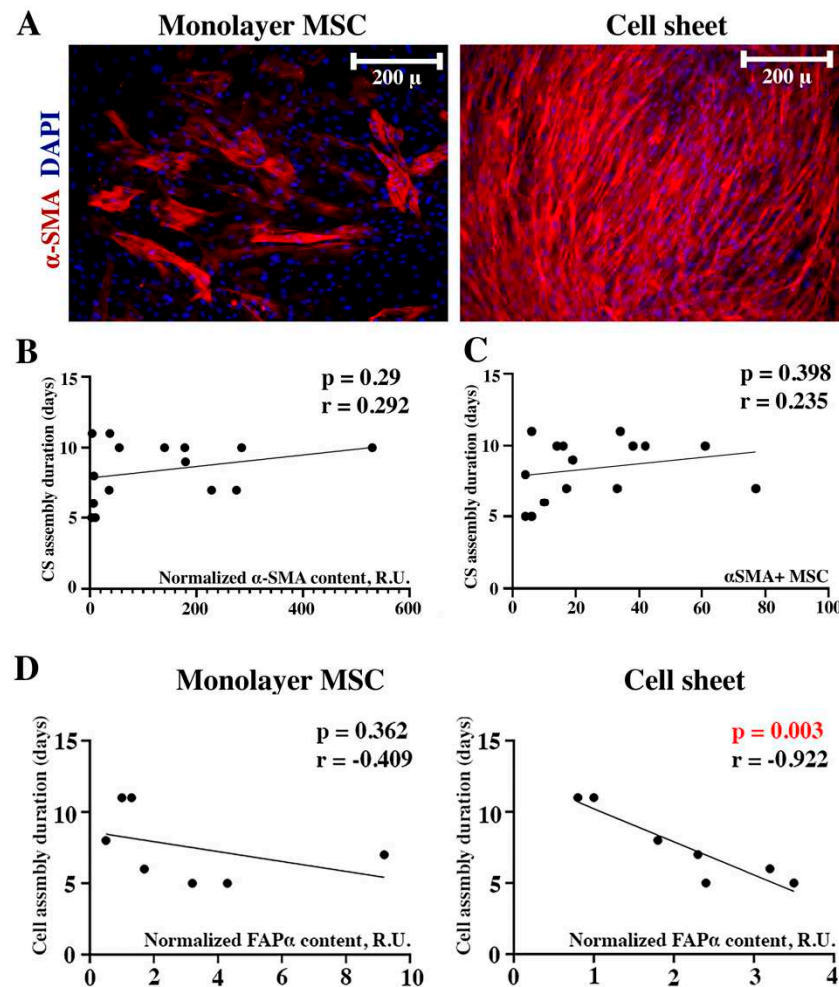
Figure 6. Evaluation of myofibroblast prevalence and FAP-α content on CS assembly duration. Immunofluorescent labeling of α-SMA in monolayer MSC and CS (A). Correlation of α-SMA contents (B) or myofibroblast counts (C) in monolayer MSC and CS assembly duration. Impact of FAP-α was detectable as an inverse correlation only in assembled CS (D) while in monolayer MSC it failed to reach statistical significance (dotted plots represent Pearson's correlations).

3.5.2. FAP-α in seeded MSC fails to correlate with CS assembly duration yet seems to be involved in its maturation at later terms

Fibroblast activating protein-α (FAP-α) is a surface serine protease expressed in developing and healing tissues playing a crucial role in regulation of stromal cells activation and ECM synthesis/turnover [15]. FAP-α was assayed in monolayer lysates and we failed to find a correlation (r=-0.409; p=0.362) between FAP-α content in monolayer MSC and CS assembly duration (Figure 7D, "Monolayer MSC"). Nevertheless, we also assayed FAP-α in assembled CS as far as this protease can modulate ECM integrity and found a strong inverse relationship (r=-0.92; p=0.003) between FAP-α contents and duration of CS assembly (Figure 7D, "Cell sheet"). Thus, despite failing to be a predictive marker for assembly duration, FAP-α increase in ready-to-use CS hints its role in ECM maturation and possible support of construct integrity.

4. Discussion

Present work was conceived to evaluate donor- and MSC-related features that impact duration of MSC sheet assembly. Comparative analysis of CS formation using parallel culture design (Supplementary Figure S1) allowed to render several interesting conclusions on the subject and

identify parameters that may determine the timing required to assembly a tissue-engineered construct.

Surprisingly, we found no correlation between CS assembly duration and basic donors' characteristics (sex and age) suggesting that cells' autonomous features retaining *in vitro* impact assembly timing stronger that individual donor parameters (Figure 2). Furthermore, this indicates that cultural conditions are sufficient to limit age-related impairments of MSC features (including proliferation rate and ECM deposition) at least in terms of efficacy of CS assembly on uncoated plastic surfaces.

Our previous data suggests active proliferation occurring at later terms of CS assembly (Days 9-12) so we expected that at early phase this would contribute to rapid formation of the construct [10].A relationship between MSC proliferation (assessed as PDT) and CS assembly time seemed obvious, but our data revealed no significant correlation between the CS assembly duration and PDT (Figure 1C). However, we were limited to PDT assessment during early-stage formation of dense monolayers which may not be relevant to later events. We suggest that transition to CS might impact the cell cycle leading to synchronization of the cell culture and modulation of division rate. Unfortunately, little is known on cell cycle changes in CS besides sporadic studies like one by Hirata et al which found a Rac1-dependent drop of proliferation and motility in sheets of keratinocytes [16]. This gap of knowledge in regards to MSC properties warrants additional studies using cell cycle imaging during CS maturation after Days 5-6 since seeding.

We also found that that MSC with a short lag–phase period acquired morphology of a ready-for-use CS (Figure 1D). This can be explained by the fact that MSCs with a substantial lag-phase take longer to adhere to plastic and accumulate solid and soluble components required to initiate mitosis. Thus, one may use assessment of lag-phase at early stages of CS assembly to receive a preliminary evaluation of expected assembly duration. Despite not being an obvious rate-limiting step, lag-phase seems a feasible parameter for evaluation at early stages of MSC culture.

Composition of ECM at early-stage MSC cultures was considered a potential predictive characteristic that might be of importance for structural formation of CS. We analyzed the major proteins that comprise interstitial matrix – collagen I and fibronectin (Figure 3) and the basement membrane proteins - collagen IV and laminin (Figures 4 and 5). Collagen I is the most abundant protein in human body accounting > 25% of all body proteins while in skin its content exceeds 60% [17]. In addition to type I collagen, high concentrations of fibronectin are also present in the ECM of connective tissues and stromal cells (including MSC) are one of major sources of mentioned components [18]. Importantly, fibronectin plays an active regulatory role in the processes associated with active proliferation of connective tissue cells - fibroblasts and MSC *in vivo* [19].

Our findings indicate that collagen I and fibronectin contents in early-stage MSC cultures seem to have opposite correlative relation with duration of CS assembly with direct correlation for collagen I reaching statistical significance. Indeed, higher contents of collagen I in MSC monolayers correlated with longer CS assembly (Figure 3). However, once we take into account our data in permeabilized monolayer cultures (Figure 3A) we may find that collagen I and not fibronectin was deposited mainly inside MSC, but not as a structural component of CS. This partially explains results of correlative semi-quantitative analysis which was conducted by dot-ELISA in lysates and cannot discern between intra- and extracellular compartments detecting total collagen I in samples. However, this does not diminish importance of using collagen I contents in monolayer MSC as a predictive marker of long- or short-term CS assembly.

Interestingly, collagen I in CS had a distinct pattern of deposition and was mostly confined to areas of high cell density (visualized by DAPI) while fibronectin (Figure 3A, "Cell sheet") was evenly distributed over the entire construct. This demonstrates differential profiles of deposition for two crucial connective tissue ECM components which correlated with our findings in CS from immortalized adipose-derived MSC (ASC52telo, ATCC, USA) [10].

Stiffness of ECM enriched by collagen I and fibronectin is often associated with mechanosensing-mediated transition of stromal cells to myofibroblasts [20]. This phenomenon is pivotal for *in vivo* wound healing due to vivid contractile ability of myofibroblasts mediated by their actin-cytoskeleton.

Its remodeling has a landmark feature of high α-smooth muscle actin (α-SMA) contents and eventually leads to wound closure and precedes activation of reparative fibrosis [21]. Nevertheless, in our study this ECM-mediated activation of transition to myofibroblasts might have played a role in CS contraction which we used as an objective event indicating completion of assembly. Our findings on α-SMA relative contents and prevalence of α-SMA-positive cells were in accordance with this assumption (Figure 6A–C) yet no correlation was found between both mentioned parameters and CS assembly duration. Dramatic increase of α-SMA-positive cells in CS was observed and can be attributed both to MSC number increase and remodeling of cytoskeleton. Our previous findings suggest that ROCK-1/2 signaling axis is of pivotal importance for CS maturation and MSC differentiation fate yet understanding of how this relates to duration of assembly is yet to be established [10].

Basement membrane proteins – collagen IV and laminin – were assessed as important components of basement membrane – a specialized ECM structure delimiting connective tissues from other cell types, providing differentiation and adhesion of cells, mechanical stability and elasticity preventing their rupture. In addition to their structural function, basement membranes provide a filter and barrier role for large molecules, and also controls cellular phenotype. Of two investigated proteins laminin provides sites for cell adhesion, and collagen IV stabilizes the entire basement membrane structure which functionally made them relevant objects influencing CS integrity and maturation. Furthermore, collagen IV and laminin bind each other via linker proteins – perlican and nidogen – which stresses their role as important structural elements of ECM.

Analysis of laminin contents revealed no correlation between its content and CS assembly duration (Figure 4). Basically, this is explained by its intracellular deposition (in both monolayer and CS) with minor presence in extracellular space. Thus, its contribution to formation of CS from monolayer MSC was of minor impact while it may but may influence other processes – e.g., organization of the basement membrane upon contact of MSCs with endothelial cells which was observed in many co-culture studies. At the same time, character of correlation of collagen IV and duration of assembly (Figure 5) we found was similar to collagen I despite its different roles in human body. While collagen I is an ubiquitous structural protein, collagen IV is confined exclusively to basement membranes [22].

Generally, our findings on laminin and collagen IV indicate that their deposition within CS play a minor role in its formation as far as majority of both were deposited intracellularly and not visualized until permeabilization (Figures 4 and 5). Nevertheless, its deposition may contribute to increase of MSC number as far as collagen IV enhances FAK-ERK signaling pathway associated with activation of MSC proliferation [23].

Evaluation of fibroblast activation protein alpha (FAP-α) was conceived to find a correlative parameter that might define MSC transition to myofibroblasts and facilitate CS maturation. However, its contents in monolayer MSC did not correlate with duration of CS assembly (Figure 6D). Its role is also attributed as a regulator of MSC migration functioning via modulation of RhoA GTPase activity while its peptidase activity is not essential for this and its inhibition did not influence migratory activity [24]. In our work we were the first to assay FAP-α in ready-to-use CS from human MSC. Our data suggests that it was higher in CS that assembled rapidly (Figure 6D) which suggests that in constructs that took less time for maturation increase of FAP-α occurs over time which was concordant with α-SMA increase in CS compared to monolayer. The mechanism of this regulatory circuit remains enigmatic yet effort is made to establish molecular pathways that connect ECM signaling and FAP-α expression in human MSC [25]. Role of FAP-α peptidase activity in ECM turnover which is possible in CS may also contribute to packaging and deposition of mature matrix proteins [26].

To conclude, our study is the first to investigate potential factors impacting CS assembly and suggests use of early-stage evaluation of ECM composition (collagen I, collagen IV) to assess the time required for completion of assembly. MSC lag-phase routine measurement can support results of ECM assays. Furthermore, we may stress that semi-quantitative dot-ELISA method is a feasible and cheap approach once data is normalized using DNA or total protein metrics. Despite descriptive

nature and certain study limitations we believe that our results are of particular interest for practical use, since they may be useful for efficient selection of cellular material in the early stages of CS assembly. It may direct further potential standardization of protocols required for CS application in tissue engineering and regenerative medicine.

References

1. Mamidi, M.K.; Singh, G.; Husin, J.M.; Nathan, K.G.; Sasidharan, G.; Zakaria, Z.; Bhonde, R.; Majumdar, A.S.; Das, A.K. Impact of passing mesenchymal stem cells through smaller bore size needles for subsequent use in patients for clinical or cosmetic indications. *J Transl Med* **2012**, *10*, 229, doi:10.1186/1479-5876-10-229.
2. Kondo, M.; Kameishi, S.; Grainger, D.W.; Okano, T. Novel therapies using cell sheets engineered from allogeneic mesenchymal stem/stromal cells. *Emerg Top Life Sci* **2020**, *4*, 677-689, doi:10.1042/ETLS20200151.
3. Yamato, M.; Okano, T. Cell sheet engineering. *Materials Today* **2004**, *7*, 42-47, doi:https://doi.org/10.1016/S1369-7021(04)00234-2.
4. Kanai, N.; Yamato, M.; Okano, T. Cell sheets engineering for esophageal regenerative medicine. *Ann Transl Med* **2014**, *2*, 28, doi:10.3978/j.issn.2305-5839.2014.03.06.
5. Cui, X.; Hartanto, Y.; Zhang, H. Advances in multicellular spheroids formation. *J R Soc Interface* **2017**, *14*, doi:10.1098/rsif.2016.0877.
6. Lin, R.Z.; Chang, H.Y. Recent advances in three-dimensional multicellular spheroid culture for biomedical research. *Biotechnol J* **2008**, *3*, 1172-1184, doi:10.1002/biot.200700228.
7. Hu, D.; Li, X.; Li, J.; Tong, P.; Li, Z.; Lin, G.; Sun, Y.; Wang, J. The preclinical and clinical progress of cell sheet engineering in regenerative medicine. *Stem Cell Res Ther* **2023**, *14*, 112, doi:10.1186/s13287-023-03340-5.
8. Lim, D.; Renteria, E.S.; Sime, D.S.; Ju, Y.M.; Kim, J.H.; Criswell, T.; Shupe, T.D.; Atala, A.; Marini, F.C.; Gurcan, M.N.; et al. Bioreactor design and validation for manufacturing strategies in tissue engineering. *Biodes Manuf* **2022**, *5*, 43-63, doi:10.1007/s42242-021-00154-3.
9. Dergilev, K.V.; Makarevich, P.I.; Tsokolaeva, Z.I.; Boldyreva, M.A.; Beloglazova, I.B.; Zubkova, E.S.; Menshikov, M.Y.; Parfyonova, Y.V. Comparison of cardiac stem cell sheets detached by Versene solution and from thermoresponsive dishes reveals similar properties of constructs. *Tissue Cell* **2017**, *49*, 64-71, doi:10.1016/j.tice.2016.12.001.
10. Nimiritsky, P.; Novoseletskaya, E.; Eremichev, R.; Alexandrushkina, N.; Karagyaur, M.; Vetrovoy, O.; Basalova, N.; Khrustaleva, A.; Tyakht, A.; Efimenko, A.; et al. Self-Organization Provides Cell Fate Commitment in MSC Sheet Condensed Areas via ROCK-Dependent Mechanism. *Biomedicines* **2021**, *9*, doi:10.3390/biomedicines9091192.
11. Alexandrushkina, N.; Nimiritsky, P.; Eremichev, R.; Popov, V.; Arbatskiy, M.; Danilova, N.; Malkov, P.; Akopyan, Z.; Tkachuk, V.; Makarevich, P. Cell Sheets from Adipose Tissue MSC Induce Healing of Pressure Ulcer and Prevent Fibrosis via Trigger Effects on Granulation Tissue Growth and Vascularization. *Int J Mol Sci* **2020**, *21*, doi:10.3390/ijms21155567.

12. Eremichev, R.; Kulebyakina, M.; Alexandrushkina, N.; Nimiritsky, P.; Basalova, N.; Grigorieva, O.; Egiazaryan, M.; Dyikanov, D.; Tkachuk, V.; Makarevich, P. Scar-Free Healing of Endometrium: Tissue-Specific Program of Stromal Cells and Its Induction by Soluble Factors Produced After Damage. *Frontiers in Cell and Developmental Biology* **2021**, *9*, doi:10.3389/fcell.2021.616893.

13. Topfer, U.; Guerra Santillan, K.Y.; Fischer-Friedrich, E.; Dahmann, C. Distinct contributions of ECM proteins to basement membrane mechanical properties in Drosophila. *Development* **2022**, *149*, doi:10.1242/dev.200456.

14. Charleux, J.; Charleux, M.; Dupont, D.; Gravagna, P.; Eloy, R.; Tardy, M.; Tayot, J.L. [Viscous human collagen IV. Physical properties and experimental tolerance]. *Ophtalmologie* **1989**, *3*, 308-311.

15. Ramirez-Montagut, T.; Blachere, N.E.; Sviderskaya, E.V.; Bennett, D.C.; Rettig, W.J.; Garin-Chesa, P.; Houghton, A.N. FAPα, a surface peptidase expressed during wound healing, is a tumor suppressor. *Oncogene* **2004**, *23*, 5435-5446, doi:10.1038/sj.onc.1207730.

16. Hirata, H.; Dobrokhotov, O.; Sokabe, M. Coordination between Cell Motility and Cell Cycle Progression in Keratinocyte Sheets via Cell-Cell Adhesion and Rac1. *iScience* **2020**, *23*, 101729, doi:10.1016/j.isci.2020.101729.

17. Magnusson, S.P.; Heinemeier, K.M.; Kjaer, M. Collagen Homeostasis and Metabolism. *Adv Exp Med Biol* **2016**, *920*, 11-25, doi:10.1007/978-3-319-33943-6_2.

18. McKee, T.J.; Perlman, G.; Morris, M.; Komarova, S.V. Extracellular matrix composition of connective tissues: a systematic review and meta-analysis. *Sci Rep* **2019**, *9*, 10542, doi:10.1038/s41598-019-46896-0.

19. Mobasseri, R.; Tian, L.; Soleimani, M.; Ramakrishna, S.; Naderi-Manesh, H. Bio-active molecules modified surfaces enhanced mesenchymal stem cell adhesion and proliferation. *Biochem Biophys Res Commun* **2017**, *483*, 312-317, doi:10.1016/j.bbrc.2016.12.146.

20. Xu, R.; Wu, M.; Wang, Y.; Li, C.; Zeng, L.; Wang, Y.; Xiao, M.; Chen, X.; Geng, S.; Lai, P.; et al. Mesenchymal stem cells reversibly de-differentiate myofibroblasts to fibroblast-like cells by inhibiting the TGF-beta-SMAD2/3 pathway. *Mol Med* **2023**, *29*, 59, doi:10.1186/s10020-023-00630-9.

21. Hinz, B.; Lagares, D. Evasion of apoptosis by myofibroblasts: a hallmark of fibrotic diseases. *Nat Rev Rheumatol* **2020**, *16*, 11-31, doi:10.1038/s41584-019-0324-5.

22. Khoshnoodi, J.; Pedchenko, V.; Hudson, B.G. Mammalian collagen IV. *Microsc Res Tech* **2008**, *71*, 357-370, doi:10.1002/jemt.20564.

23. Shudo, Y.; Cohen, J.E.; Goldstone, A.B.; MacArthur, J.W.; Patel, J.; Edwards, B.B.; Hopkins, M.S.; Steele, A.N.; Joubert, L.M.; Miyagawa, S.; et al. Isolation and trans-differentiation of mesenchymal stromal cells into smooth muscle cells: Utility and applicability for cell-sheet engineering. *Cytotherapy* **2016**, *18*, 510-517, doi:10.1016/j.jcyt.2016.01.012.

24. Chung, K.M.; Hsu, S.C.; Chu, Y.R.; Lin, M.Y.; Jiaang, W.T.; Chen, R.H.; Chen, X. Fibroblast activation protein (FAP) is essential for the migration of bone marrow mesenchymal stem cells through RhoA activation. *PLoS One* **2014**, *9*, e88772, doi:10.1371/journal.pone.0088772.

25. Bae, S.; Park, C.W.; Son, H.K.; Ju, H.K.; Paik, D.; Jeon, C.J.; Koh, G.Y.; Kim, J.; Kim, H. Fibroblast activation protein alpha identifies mesenchymal stromal cells from human bone marrow. *Br J Haematol* **2008**, *142*, 827-830, doi:10.1111/j.1365-2141.2008.07241.x.

26. Fan, M.H.; Zhu, Q.; Li, H.H.; Ra, H.J.; Majumdar, S.; Gulick, D.L.; Jerome, J.A.; Madsen, D.H.; Christofidou-Solomidou, M.; Speicher, D.W.; et al. Fibroblast Activation Protein (FAP) Accelerates Collagen Degradation and Clearance from Lungs in Mice. *J Biol Chem* **2016**, *291*, 8070-8089, doi:10.1074/jbc.M115.701433.